Longitudinal, Degenerate, and Transversal Parametric Oscillation in Photorefractive Media

Henrik C. Pedersen* and Per Michael Johansen

Optics and Fluid Dynamics Department, Risø National Laboratory, DK-4000 Roskilde, Denmark

(Received 17 June 1996)

We present a theoretical model of photorefractive parametric oscillation that covers, for the first time, to our knowledge, the occurrence of the whole spectrum of parametric processes from transversal over degenerate to longitudinal parametric oscillation. It is shown that inclusion of so-called noneigenwaves is essential for completing the model. We report on the first experiment that shows the transition from transversal over degenerate to longitudinal parametric oscillation. The experimental observations agree well with the theoretical predictions. [S0031-9007(96)01360-9]

PACS numbers: 42.65.Hw, 42.70.Nq, 52.35.Mw

Photorefractive parametric oscillation is a nonlinear instability process that might appear when a running holographic grating is recorded in a photorefractive crystal [1]. These types of processes are closely connected to the recently discovered parametric amplification processes [2]. For certain grating velocities the grating becomes unstable against excitation of two secondary gratings referred to as signal and idler gratings and we have the state of parametric oscillation. The originally induced running grating is then referred to as the pump grating which transfers grating strength to the signal and idler gratings. To obtain the necessary nonlinear coupling between the three gratings the so-called spatial synchronism condition [3] $\vec{k}_S + \vec{k}_I = \vec{k}_P$ has to be fulfilled, where $\vec{k}_S$, $\vec{k}_I$, and $\vec{k}_P$ are the signal, idler, and pump grating vectors, respectively. Degenerate parametric oscillation (DPO) refers to the case where the signal and idler gratings are identical; hence, $\vec{k}_S = \vec{k}_I = \vec{k}_P/2$. This is also referred to as ordinary subharmonic generation. Contrary to this, longitudinal parametric oscillation (LPO) and transversal parametric oscillation (TPO) are nondegenerate processes where $\vec{k}_S \neq \vec{k}_I$. In the case of LPO $\vec{k}_S$ and $\vec{k}_I$ are both aligned along the fundamental grating vector $\vec{k}_P$. This process was theoretically predicted by Sturman *et al.* [3] and to some extent experimentally verified by Pedersen and Johansen [1]. In the case of TPO $\vec{k}_S$, $\vec{k}_I$, and $\vec{k}_P$ are all noncollinear. This process has been reported on only once [4] but similar observations had been done a few years before by a group in Oxford [5]. To the best of our knowledge, no previous theory has been able to explain the occurrence of TPO. Neither has it been clarified experimentally for which parameters the individual parametric processes appear. These questions are clarified both theoretically and experimentally in this Letter.

The theoretical basis is the nonlinear wave equation which governs the induced waves of space-charge field $\vec{E}_1(\vec{r}, t)$, when a photorefractive crystal is illuminated by the light intensity distribution $I(\vec{r}, t) = I_0 + I_1(\vec{r}, t)$ [1,3]:

$$\vec{E}_0 \cdot (\nabla^2 \dot{\vec{E}}_1) + \frac{k_B T}{q} \vec{\nabla} \cdot (\nabla^2 \dot{\vec{E}}_1) + \omega_0 \vec{E}_0 \cdot (\nabla^2 \vec{E}_1) + \frac{k_B T}{q} \omega_0 \vec{\nabla} \cdot (\nabla^2 \vec{E}_1) - \zeta I_0 \vec{\nabla} \cdot \vec{E}_1 - \frac{1}{\mu\tau} \vec{\nabla} \cdot \dot{\vec{E}}_1$$
$$= \zeta \vec{E}_0 \cdot (\vec{\nabla} I_1) + \frac{k_B T}{q} \zeta \nabla^2 I_1 + \zeta \vec{\nabla} \cdot (I_1 \vec{E}_1) - \omega_0 \vec{\nabla} \cdot [\vec{E}_1 (\vec{\nabla} \cdot \vec{E}_1)] - \vec{\nabla} \cdot [\vec{E}_1 (\vec{\nabla} \cdot \dot{\vec{E}}_1)], \quad (1)$$

where the explicit dependencies of $\vec{E}_1$ and I_1 on $\vec{r}$ and t are omitted for simplicity. $\vec{E}_0$ is a constant electric field that has to be applied to the medium in order to observe the parametric effects. k_B is the Boltzmann constant, T is the absolute temperature, q is the absolute value of the electronic charge, I_0 is the spatially averaged light intensity, μ is the mobility of conduction band electrons, and τ is the electron recombination time given by $\tau = (\gamma_R N_A)^{-1}$, where γ_R is the recombination constant and N_A is the density of acceptors. The two constants ω_0 and ζ are given by $\omega_0 = sI_0 N_D/N_A$ and $\zeta = sqN_D/\varepsilon_0\varepsilon_S$, where s is the photoexcitation cross section, N_D is the total density of donors, and $\varepsilon_0\varepsilon_S$ is the permittivity of the crystal.

The wave equation is seen to include three quadratic nonlinear terms which are doubly underlined on the right hand side. These are responsible for the parametric processes in photorefractive media. We now want to consider the stability of the induced fundamental space-charge field when the photorefractive medium is illuminated by the intensity distribution $I_1 = mI_0 \cos(k_P x - \Omega t)$, where m is the intensity modulation coefficient, k_P is the fringe wave number, and Ω is the temporal, angular frequency of the running fringe pattern. The electric field $\vec{E}_0$ is applied perpendicular to the intensity fringe planes.

In the model of Sturman *et al.* [3] it is assumed that the secondary grating waves fulfill the linear dispersion relation of the medium. In our model we make no prerequisites in this respect; hence, we use as a solution ansatz of the form

$$\vec{E}_1 = \hat{x}\mathcal{E}_P \exp(ik_P x - i\Omega t) + \hat{k}_S \mathcal{E}_S(t) \exp(i\vec{k}_S \cdot \vec{r}) + \hat{k}_I \mathcal{E}_I(t) \exp(i\vec{k}_I \cdot \vec{r}) + \text{c.c.}, \quad (2)$$

 0031-9007/96/77(15)/3106(4)$10.00

where $\hat{x}$, $\hat{k}_S$, and $\hat{k}_I$ are unit vectors along the x axis, $\vec{k}_S$, and $\vec{k}_I$, respectively. $\mathcal{E}_P$, $\mathcal{E}_S$, and $\mathcal{E}_I$ are the fundamental (pump), signal, and idler space-charge field amplitudes and c.c. denotes the complex conjugate. $\mathcal{E}_P$ is taken as the linear solution to Eq. (2) which we assume to be slowly varying in the very first period of time where $\mathcal{E}_S$ and $\mathcal{E}_I$ may start to grow. As is seen we make no assumptions about the temporal frequencies of the secondary waves; thus we include eigenwaves as well as noneigenwaves in the analysis. Inserting the ansatz (2) into Eq. (1) and neglecting higher order terms we obtain the following linear set of coupled amplitude equations:

$$\begin{aligned} \dot{\mathcal{E}}_S + A_S \mathcal{E}_S &= B_S \tilde{\mathcal{E}}_I^* + C_S \dot{\tilde{\mathcal{E}}}_I^*, \\ \dot{\tilde{\mathcal{E}}}_I^* + A_I^* \tilde{\mathcal{E}}_I^* &= B_I^* \mathcal{E}_S + C_I^* \dot{\mathcal{E}}_S, \end{aligned} \tag{3}$$

where

$$\begin{aligned} &\tilde{\mathcal{E}}_I = \mathcal{E}_I \exp(i\Omega t), \qquad A_S = \gamma_{\vec{k}_S} + i\omega_{\vec{k}_S}, \qquad A_I^* = \gamma_{\vec{k}_I} - i(\omega_{\vec{k}_I} - \Omega), \\ &B_S = \frac{-\frac{1}{2} m\omega_0 E_{q,\vec{k}_S} \nu_1 + [(\Omega + i\omega_0) X^{-1} \nu_1 + (\Omega - i\omega_0)\nu_2]\mathcal{E}_P}{E_{D,\vec{k}_S} + E_{M,\vec{k}_S} - iE_0} \\ &B_I^* = \frac{-\frac{1}{2} m\omega_0 E_{q,\vec{k}_I} \nu_1 + [(\Omega + i\omega_0)(1 - X)^{-1} \nu_1 + i\omega_0 \nu_2^{-1}]\mathcal{E}_P^*}{E_{D,\vec{k}_I} + E_{M,\vec{k}_I} + iE_0}, \\ &C_S = -i \frac{\mathcal{E}_P}{E_{D,\vec{k}_S} + E_{M,\vec{k}_S} - iE_0} \nu_2, \qquad C_I^* = i \frac{\mathcal{E}_P^*}{E_{D,\vec{k}_I} + E_{M,\vec{k}_I} + iE_0} \nu_2^{-1}, \\ &\nu_1 = \frac{X(1 - X) - Y^2}{\sqrt{X^2 + Y^2}\sqrt{(1 - X)^2 + Y^2}}, \qquad \nu_2 = \frac{\sqrt{(1 - X)^2 + Y^2}}{\sqrt{X^2 + Y^2}}, \qquad X = \frac{k_{S\parallel}}{k_P}, \qquad Y = \frac{k_{S\perp}}{k_P}. \end{aligned} \tag{4}$$

$\gamma_{\vec{k}_I}$ and $\omega_{\vec{k}_I}$ are the damping factors and eigenfrequencies of the grating waves and $E_{D,\vec{k}_I}$, $E_{q,\vec{k}_I}$, and $E_{M,\vec{k}_I}$ are the characteristic photorefractive diffusion, saturation, and drift fields, respectively [3]. $k_{S\parallel}$ and $k_{S\perp}$ are the components of $\vec{k}_S$ that are, respectively, parallel and perpendicular to $\vec{E}_0$. The characteristic exponents of Eqs. (3) are found to be

$$s_\pm = -Q_1 \pm \sqrt{Q_1^2 - Q_2}, \tag{5}$$

where

$$\begin{aligned} Q_1 &= \frac{1}{2} \frac{A_S + A_I^* - B_S C_I^* - B_I^* C_S}{1 - C_S C_I^*}, \\ Q_2 &= \frac{A_S A_I^* - B_S B_I^*}{1 - C_S C_I^*}. \end{aligned} \tag{6}$$

Because $\mathcal{E}_S$ and $\tilde{\mathcal{E}}_I^*$ are proportional to $\exp(s_\pm t)$ we wish to find out for which parameters s_+ and s_- have positive real parts; in these cases the fundamental wave becomes unstable against excitation of the signal and idler waves and, hence, we have parametric oscillation. Inasmuch as the real part of s_- is always less than the real part of s_+ we need only consider the latter.

In Fig. 1 the real part of s_+ is plotted versus X and Y for different values of the detuning parameter ε given by $\omega_{\vec{k}_P}/\Omega$, where $\omega_{\vec{k}_P}$ is the eigenfrequency of the fundamental wave [3]. The fundamental wave vector assumes the coordinates $(X, Y) = (1, 0)$. For each point (X, Y) that is inside the dashed contour, a signal wave with wave vector $(X, Y)k_P$ and an idler wave with wave vector $(1 - X, -Y)k_P$ can occur in the medium.

Starting at $\varepsilon = 2$ it is seen that an instability region centered at $X = 0.5$ and $Y = 0$ appears. The center corresponds to the case of DPO. When ε is reduced the system enters a state of TPO where the signal and idler wave

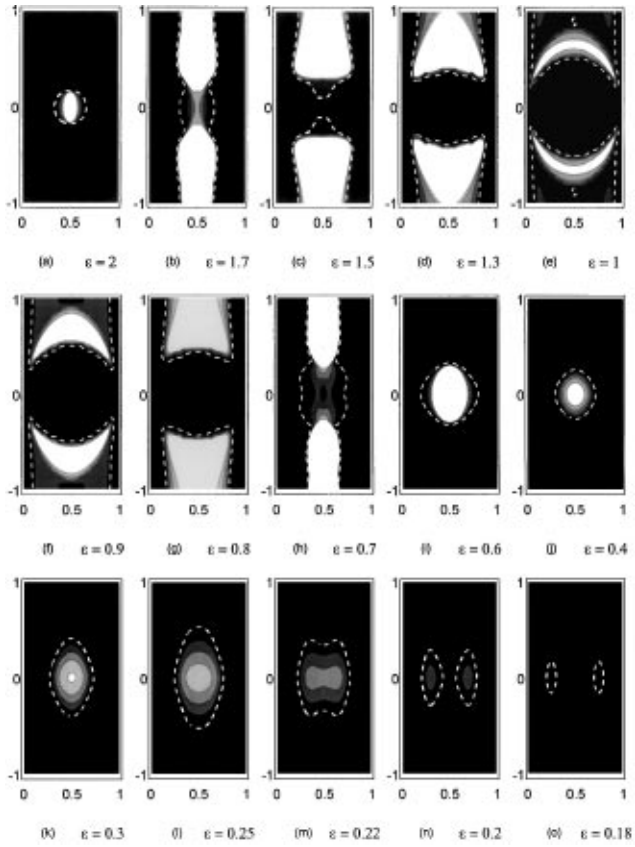

FIG. 1. Contour plots of the real part of s_+ versus X (abscissa) and Y (ordinate) for different values of ε. In all cases the light areas represent regions of instability; the black areas represent stable regions. The dashed contour represents $\mathrm{Re}\{s_+\} = 0$; the subsequent contours represent $\mathrm{Re}\{s_+\} = 5$, 10, 15, and 20 s^{-1}, respectively. The following parameters are used: $E_0 = 14$ kV/cm, $k_P = 2\pi/30\ \mu\mathrm{m}^{-1}$, $I_0 = 40.7$ mW/cm^2 along with crystal parameters relevant to BSO [1].

vectors are nonparallel to $\vec{k}_P$. Decreasing ε further the system reenters a region of DPO, and then for $0.22 > \varepsilon > 0.18$, LPO arises where the instability region splits up along the longitudinal direction. It is seen that the instabilities are much stronger for TPO and DPO than for LPO.

The first interesting aspect of Fig. 1 is that for every value of ε it is possible for a whole continuum of secondary waves to be excited, not only one pair. This is opposed to the model of Sturman *et al.* [3] which predicts that for each value of ε only one particular longitudinal component for $\vec{k}_S$ and one for $\vec{k}_I$ are possible. Hence, one of the results of not forcing the secondary waves to be eigenwaves is the emergence of a two-dimensional continuum of secondary waves. The next new finding of Fig. 1 is the instability regions that appear for $\varepsilon > 0.25$. Again, this is opposed to the results of Ref. [3], where it was concluded that no instability could be found in this region. However, as is seen, it is in this very region that TPO is found.

To support the theoretical results we have performed a series of experiments in a crystal of BSO. A schematic representation of the setup used is shown in Fig. 2. Two collimated and linearly polarized recording beams from an Ar^+ laser at 514.5 nm are illuminating the crystal in a way so that the interference fringes are perpendicular to the x axis. The crystal used here has the dimensions $5 \times 10 \times 10$ mm along the x, y, and z axes, respectively. The recording beams have equal intensities of $20.35\ \mathrm{mW/cm^2}$. One of the beams is shifted in frequency by an amount Ω due to reflection from a moving piezomirror. The two recording beams form a running interference pattern with the modulation coefficient $m = 1$ and a spatial period of $\Lambda_P = 30\ \mu$m. Moreover, a dc electric field of $14\ \mathrm{kV/cm}$ is applied along the x axis. The induced holograms are read out by a 7 mW linearly y polarized HeNe laser at 632.8 nm. The diffraction patterns are projected on a screen from where a charge coupled device camera records the patterns.

At first, the frequency shift Ω at which the fundamental grating has maximum strength is measured. At this value $\Omega = \omega_{\vec{k}_P}$, i.e., $\varepsilon = 1$. To avoid so-called nonlinear frequency shift [6] the modulation coefficient is provisionally decreased to 0.21 after which maximum diffraction efficiency is obtained at $\Omega = \omega_{\vec{k}_P} = 88\ \mathrm{s^{-1}}$. In the following this value is used as a basis for determination of ε.

m is now reset to 1 and the readout angle is adjusted to Bragg match an eventual $\vec{k}_P/2$ grating. One should note that because of the large grating fringe spacings involved here (>30 μm) the angular Bragg selectivity is very poor. Therefore, also the fundamental grating is read out in this configuration plus all additional gratings with fringe spacings larger than the fundamental one that might appear when the fundamental grating becomes unstable. By gradually increasing Ω, ε is now varied from 0.48 down to 0.06. Thereby, the diffraction patterns shown in Figs. 3(a)–3(t) appear on the screen.

When starting to decrease ε from 0.48 and downwards it is seen that some secondary gratings appear with grating vectors spread around $\vec{k}_P/2$ [Figs. 3(a)–3(c)]. Then at $\varepsilon = 0.38$ the diffraction pattern starts splitting up into two spots along the transversal direction (i.e., along the y axis). The splitting becomes more and more pronounced as ε runs through the interval $0.38 > \varepsilon > 0.29$. Hence, in this interval we have clear experimental evidence of TPO. For $0.23 > \varepsilon > 0.13$ a continuous evolution from TPO to DPO is observed; see Figs. 3(j)–3(n). At $\varepsilon = 0.11$, we observe a pure case of DPO. When decreasing ε further the central $\vec{k}_P/2$ spot starts to broaden, this time in the longitudinal direction (i.e., along the x axis) ending up with a longitudinal splitting of the spot, first into three spots ($\varepsilon = 0.08$) and then into two spots ($\varepsilon = 0.07$). Hence, the process has developed into LPO.

By comparing Figs. 1 and 3 it is seen that generally quite good qualitative agreement is obtained between instability regions (Fig. 1) and regions that are occupied by signal-idler pairs in steady state (Fig. 3). Except for the DPO region at high ε values in Fig. 1 both sets

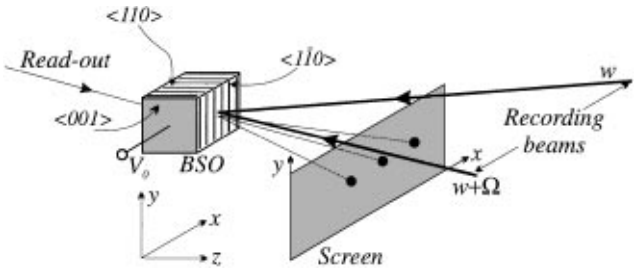

FIG. 2. Schematic diagram of the experimental setup used for observation of parametric oscillation in a crystal of BSO. The plane formed by the recording beams and the plane formed by the diffracted readout beams are slightly tilted with respect to one another (approximately 2°) in order to separate the readout beams from the recording beams.

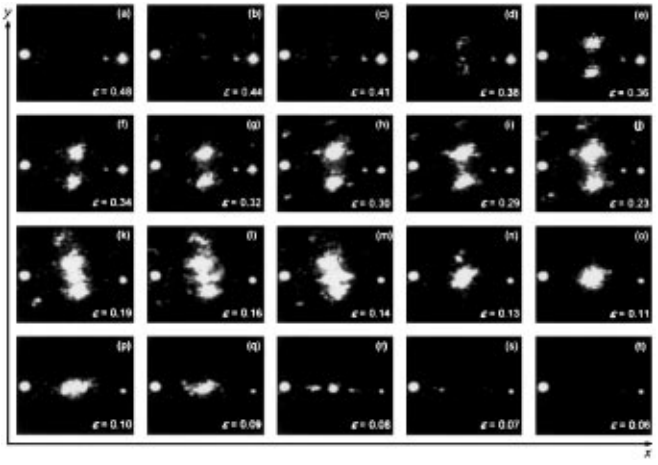

FIG. 3. Diffraction patterns observed on the screen for different values of ε. In all pictures the powerful spot on the left is the directly transmitted spot (zeroth order) whereas the spot on the right is the first order spot. All spots in between stem from diffraction in secondary gratings that arise due to parametric oscillation.

of figures show that as ε is decreased the parametric instability process goes from TPO over DPO to LPO. To our knowledge, this has never been demonstrated before. It is also seen that the gratings of TPO and DPO are much stronger than those for LPO. This agrees also well with the results in Fig. 1.

If one compares the different values of ε in Figs. 1 and 3 it is seen that the theoretical values are generally higher than the corresponding experimental ones. Moreover, the experimental pictures show that TPO and DPO appear simultaneously for a broad interval of ε; the theoretical results show that only within a narrow region around $\varepsilon = 1.7$ and 0.7 this can happen. How can we explain these contradictions? The answer is that absorption of the recording beams causes I_0 and thereby ε to vary exponentially along the z axis. The absorption coefficient in the crystal used here was measured to 1.4 cm^{-1}. This implies that at the front surface, where the recording beams enter the crystal, ε is about four times larger than at the back surface. Thus, for a certain value of Ω, ε might, for example, equal 1 at the front end of the crystal and 0.25 at the rear end. As a result, all processes from Figs. 1(e) to 1(l) will appear within the length of the crystal. Since readout is performed along the z axis, all processes are read out simultaneously and, hence, we observe pictures like Figs. 3(j)–3(n) where both TPO and DPO appear. For the same reason the experimental values of ε given in Fig. 3 are not exact in the sense that they are average values where the averaging is performed along the z axis over the entire length of the crystal. Consequently, one cannot quantitatively compare the values of ε in Figs. 1 and 3.

In conclusion, we have presented the first theoretical model that is capable of describing the occurrence of transversal parametric oscillation. It is shown both theoretically and experimentally that as the detuning parameter ε is decreased the parametric process evolves from transversal over degenerate to longitudinal parametric oscillation.

This work was supported by the Danish Natural Science Research Council, Grant No. 9502764.

*Electronic address: LAS-HCPE@RISOE.DK

[1] H. C. Pedersen and P. M. Johansen, J. Opt. Soc. Am. B **12**, 1065 (1995).
[2] H. C. Pedersen and P. M. Johansen, Phys. Rev. Lett. **76**, 4159 (1996).
[3] B. I. Sturman, M. Mann, and K. H. Ringhofer, Appl. Phys. A **55**, 235 (1992); B. I. Sturman, M. Mann, J. Otten, and K. H. Ringhofer, J. Opt. Soc. Am. B **10**, 1919 (1993).
[4] H. C. Pedersen and P. M. Johansen, Opt. Lett. **19**, 1418 (1994).
[5] J. Takacs and L. Solymar (private communication).
[6] T. E. McClelland, D. J. Webb, B. I. Sturman, M. Mann, and K. H. Ringhofer, Opt. Commun. **113**, 371 (1995).